



## RESEARCH ARTICLE - ENGINEERING

# Grid-Connected PV System for 324 kW with Improved Maximum PowerPoint Tracking

Abbas Hussein Khariy<sup>1\*</sup>, Ahmed Rashid Ajel<sup>1</sup>, Sadik Kamel Gharghan<sup>1</sup>, Noaman Mohammad Noaman<sup>2</sup>

<sup>1</sup>Electrical Engineering Technical College, Middle Technical University, Baghdad, Iraq

<sup>2</sup>College of Engineering, University of Technology Bahrain, Bahrain

\* Corresponding author E-mail: [bcc0010@mtu.edu.iq](mailto:bcc0010@mtu.edu.iq)

Article Info.	Abstract
<p><i>Article history:</i></p> <p>Received 12 July 2022</p> <p>Accepted 09 October 2022</p> <p>Publishing 30 June 2023</p>	<p>The purpose of this work is to analyze and studied, a grid-connected with a double-stage converter DC/DC, a three-phase five-level inverter system, battery energy system (BESS) with dynamic and static load. A DC/DC modified boost converter is used to get to most power out of the photovoltaic array along with increasing output voltage. The duty cycle is changed in an incremental conductance maximum power point tracking (MPPT) technique to reach the maximum power point (MPP). In a rotating d-q synchronous reference frame, the multilevel voltage source inverter converts the maximum voltage (VSI). power obtained from first stage power converter (DC-DC) to AC power utilizing a droop controller approach. Finally, the simulation results demonstrated the effectiveness of the proposed modified MPPT strategy for tracking the maximum power under shading conditions with an accuracy of up to 98.5%. The suggested AC controller results also show robust performance for synchronizing with the utility grid with a minimum THD of up to 2.4%.</p>
<p>This is an open-access article under the CC BY 4.0 license (<a href="http://creativecommons.org/licenses/by/4.0/">http://creativecommons.org/licenses/by/4.0/</a>)</p>	
<p>Publisher : Middle Technical University</p>	
<p><b>Keywords:</b> Grid-Connected; PV Systems; MPPT.</p>	

## 1. Introduction

The two renewable energy sources that are expanding the fastest are solar and wind energy [1]. Since the PV system cannot be connected directly to the load, its full potential won't be realized. Between the PV source and the load, an electronic controller is required for optimal PV source consumption under all operational situations [2]. The PV system's energy efficiency can be increased by operating the PV source at its maximum power point (MPP), thanks to this electronic controller. Numerous control techniques, including incremental conductance (INC), adaptive neuro-fuzzy inference system (ANFIS), and perturbation and observation, have been documented in the literature to track the maximum power from the PV arrays (P&O).

Maximum power point tracking is provided by the fractional PID and INC algorithm calculation requirements [3]. Different DC-DC converter topologies can track the MPP in a PV-generating system. An LCD voltage multiplier cell has been used in place of the boost converter's inductor, and it is provided as a converter [4]. These converters' high gain, reduced current ripple, reduced heating, and reduced losses are a few of their main benefits. In the last ten years, multilevel inverters have gained popularity in academics and industry for high-power and medium-voltage energy control. They can also create switching waveforms with reduced harmonic distortion when compared to a two-level converter sinusoidal pulse width modulation, multilayer selective harmonic synthesizer with a comparable rating. The output waveform's harmonic distortion is reduced by the multilayer idea without affecting the inverter's power output. The three most significant topologies are presented in this study [5]: diode-clamped inverter, capacitor-clamped, and cascaded multilevel with distinct dc sources (flying capacitor). The most pertinent modulation techniques created for this converter family are also presented in this study. Space-vector modulation, multilevel selective harmonic removal, and multilayer sinusoidal pulse width modulation.

The 95% of solar PV inverters intended for use-interconnected operation should perform to perfect power factor and to get less than 5% from THD current at rated of output power inverter, PV system utility interface according to IEEE standard 929-2000 [5]. The performance of solar PV systems, as well as other variables such as Power quality, consistency, and dependability, determine their activity and also have advantages and disadvantages shown in Table 1. To comprehend the performance of a grid-connected PV system, it is also necessary to evaluate the payback period and profitability from the aspect of investment. [6].

Many research and development initiatives have been conducted in this manner to progress and optimize the solar PV systems used.

Nomenclature & Symbols			
AC	Alternating Current	PCU	Power Conditioning Unit
ANFIS	Adaptive Neuro-Fuzzy Inference System	PLL	Phase-Locked Loop
BESS	Battery Energy Storage	PCC	Point Of Common Connection
CCPWM	Current Control Plus Modulation	UPF	Unity Power Factor
DC	Direct Current	VSI	Voltage Source Inverter
FOPID	Fractional Order PID	$\lambda$	Integral Order
INC	Incremental Conductance	$\mu$	Derivative Order
MPPT	Maximum Power Point Tracking	$I_{ing}$	Injected Current (A)
THD	Total Harmonic Distortion	$I_{sh}$	Short Circuit Current (A)
PV	Photovoltaic	$V_{oc}$	Open Circuit Voltage (V)

The purpose of this work is to assess the activity of a 324 KW PV system grid-connected when utilized as a DG system with nonlinear loads. The major goals are to maximize the output power from the PV argument and to balance the power by injecting AC power with high quality into the grid by IEEE 929-2000 standards (THD, ripple less than 005, osculation  $\leq 0.01$ ) and synchronize with grid same frequency, phase angle, and amplitude voltage. It also includes a review of system performance in terms of MPPT efficiency, total conversion efficiency, control strategy, and grid functionality.

Table 1. Advantages and disadvantages of Solar Energy

Advantages of Solar Energy	Disadvantages of Solar Energy
Reduces Electricity Bills	Weather Dependent
Diverse Applications	Solar Energy Storage is Expensive
Low Maintenance Costs	Uses a Lot of Space
Technology Development	Associated with Pollution

## 2. Literature Review

### 2.1. Henry Massawe, 2013

Study a laboratory project on renewable energy, "Grid Connected PV Systems with Smart Grid Functionality,". It treats and fixed the case of shadowing PV modules. He focused on the power stage of the PV-grid concentrated inverter stage, which is needed to support the proposed PV system under consideration. Power stage inverter parameters are estimated and proposed. a single-phase, one-kilowatt, 230-volt, two-power-stage inverter, the boost inductor and the input capacitor are calculated as two t components of the boost inductor (VSI). The L-C-L filter and a switching strategy are presented to provide a clear sinusoidal output phase voltage of 230V from a DC capacitance bus that can tolerate 400V. The result is a more efficient and reliable PV system [7].

### 2.2. Ali Bouhafs Bendaas Mohamed Lokmane, 2015

The purpose of this study is to look at a huge three-phase inverter system that is connected to the grid. A three-phase grid-connected inverter for an 800W photovoltaic system will be demonstrated. The converter uses to increase the output voltage of the photovoltaic array and to implement maximum power point tracking by incremental technique. A three-phase, two-level VSI was utilized to increase the PV system's conversion efficiency, which is significantly influenced by the transformer main voltage and DC link voltage, to inject a high-quality AC into the grid. The total conversion efficiency grew as the transformer's primary voltage increased [8].

### 2.3. Ann Arbor; 2016

A unique power management system described in this thesis controls the voltage source converter (VSC), battery charging and discharging, and PV (MPPT) generation in PV-battery systems. The power flow between the PV system, the battery, and the utility grid can be balanced with the proposed control system. The result of the proposed control strategy has two advantages;

- The DC bus voltage on the system is stable and adjustable, making it simple to connect other DC devices to it.
- The system reacts to power changes in the DC microgrid more quickly [9].

### 2.4. Amirreza Naderipour, Zulkurnain Abdul-Malek, and Vigna K. Ramchandaramurthy, 2019

A compensation approach for a grid-connected PV inverter using a unity power factor strategy is investigated in this work (UPF). Simulation data and theoretical analysis are used to assess the performance of the proposed control mechanism in a microgrid with a grid-connected inverter. It can raise the output current of the inverter by over 19 times the value reached using traditional methods [10].

### 2.5. Aravind Khote, Shalini Goad; 2021

In this research, the incremental conductance approach and the genetic algorithm-based method for MPPT simulated by MATLAB-Simulink are compared. In this experiment, variable irradiation and temperature are used. The ANFIS MPPT methodology delivers a boost converted output voltage of 502.13 V for ANFIS, while the INC MPPT method produces a boost converted output voltage of 501.50 V, according to the simulation data. Furthermore, the output power of a boost converter for variable irradiation is 92.26 KW for ANFIS and 90.41 KW for INC, according to just comparison data. The results clearly show that the ANFIS technique is superior to INC in terms of consistent irradiation [11].

### 3. Research Methodology

#### 3.1. PV System and PV sizing

PV panels and equipment for power conditions, such as a DC/DC, MPPT technical, inverter DC/AC, and filters, are among the different components of a PV system. A DC-DC modified boost converter boosts up the output DC-generated voltage to the required voltage since the output voltage is variable and low. Weather conditions determine the amount of PV power generated [12]. there is a single operational point on the I-V and P-V curve when the PV panels' generated output power is at its maximum, which is denoted by p max in Fig. 1. An MMPT controller with a fractional PID controller is used to track one of a kind operational point. Currently, the PV system is controlled by the storage system battery, which also manages the power balance between photovoltaic power and microgrid [13].

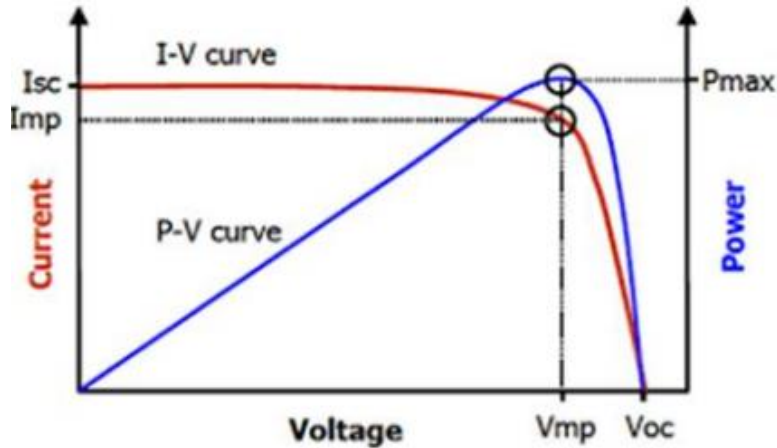


Fig. 1. The photovoltaic cell characteristic (I-V curves) [13]

The layout configuration in this work is shown in Fig. 2, all main parts used in the build of the PV system grid-connected.

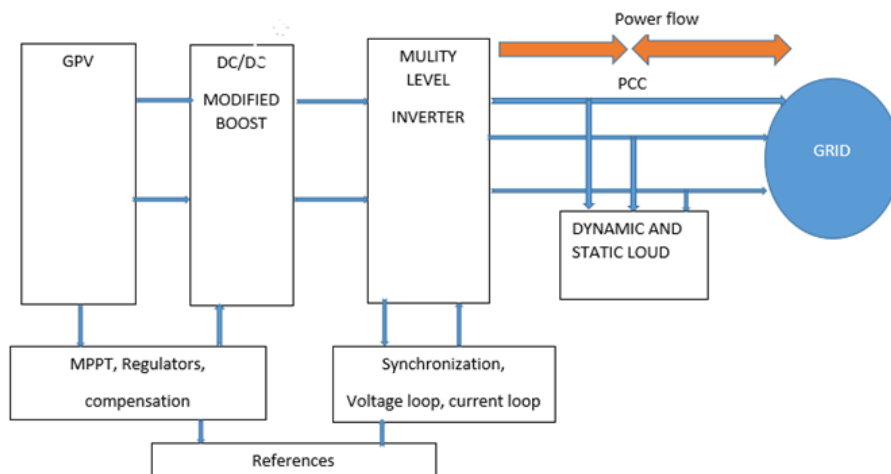


Fig. 2. General Topology of a grid-connected photovoltaic system

In this paper can be calculated the PV sizing for an agricultural research center shown in Fig. 3, with a total load of 2106 kWh and use module of Vertex with electrical data as shown in Table 2:

- Total power =  $(total\ energy)/(sun\ arc\ hours)$  ➡ Total power =  $(2106kwh/6.5h)$  ➡ Total power= 324kw
- PV module output power = 405 W. ➡ No. of PV module =  $(Total\ power)/(PV\ module\ power\ output)$

No. of PV module=  $324kw/405w = 800\ pcs$

Table 2. Electrical Data (Stc) [Back sheet Monocrystalline Module of Vertex: Tsm-De19]

Parameter	Specification
Open circuit voltage (Voc)	35.1 V
Maximum power voltage	28.8 V
Scct current (Isc)	14.8 A
Max current	14.06 A
P max	405W
Coefficient of temperature at any power (C)	0.34%
Number of serial models	20
Number of parallel modules	40
Total modules	800 pcs

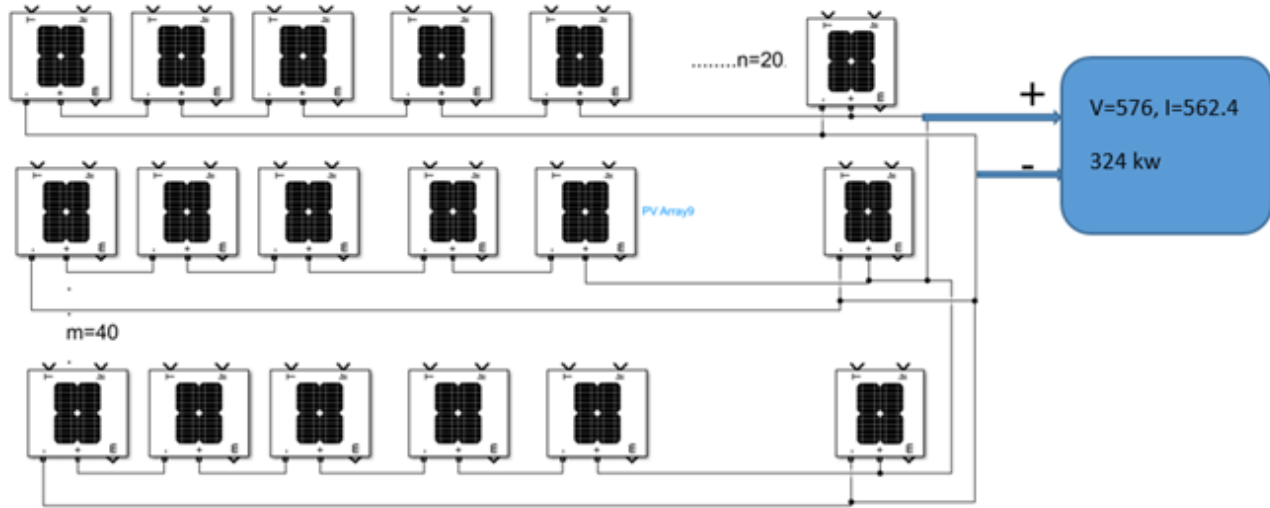


Fig. 3. Layout of the PV panel system connection to verify the generation of 324kw

3.2. Battery sizing

- $V_{dc} = (2\sqrt{2} vll) / (\sqrt{3} \times 0.83) \Rightarrow V_{dc} = (2\sqrt{2} \times 400) / (\sqrt{3} \times 0.83) \Rightarrow V_{dc} = 786.984 \approx 800 \text{ v}$
- battery capacity =  $\frac{\text{Day of autonomy} \times \text{Total energy}}{\text{Depth of discharge} \times \text{Coefficient factor of temperature} \times V_{dc}}$  battery capacity =  $(3 \times 2106000 / 800) / (0.7 \times 0.95) \Rightarrow$  battery capacity =  $11875.93 \text{ A/h}$
- no. of battery using in series stray =  $V_{dc} / (V \text{ battery}) = 800 / 48 = 16.66 \approx 17 \text{ pcs}$
- Capacity of battery =  $400 \text{ A/h}$
- The capacity of the battery with preparation ratio =  $400 / 0.16 = 2500 \text{ A/h}$
- No. of string battery in parallel stray =  $11875.93 / 2500 = 4.75 \approx 5$

3.3. DC/DC converter

A modified boost converter with a voltage multiplier cell is offered as a converter Fig. 4(a). An LCD voltage multiplier cell has been used in place of the boost converter's inductor, as seen in Fig. 4(a). In addition, in the final portion, a voltage double was used. The function of the suggested converter is divided into two modes. To explain how each mode of operation works with the proposed converter [14].

$V_{L1} = V_{L2} = V_{IN}$

(1)

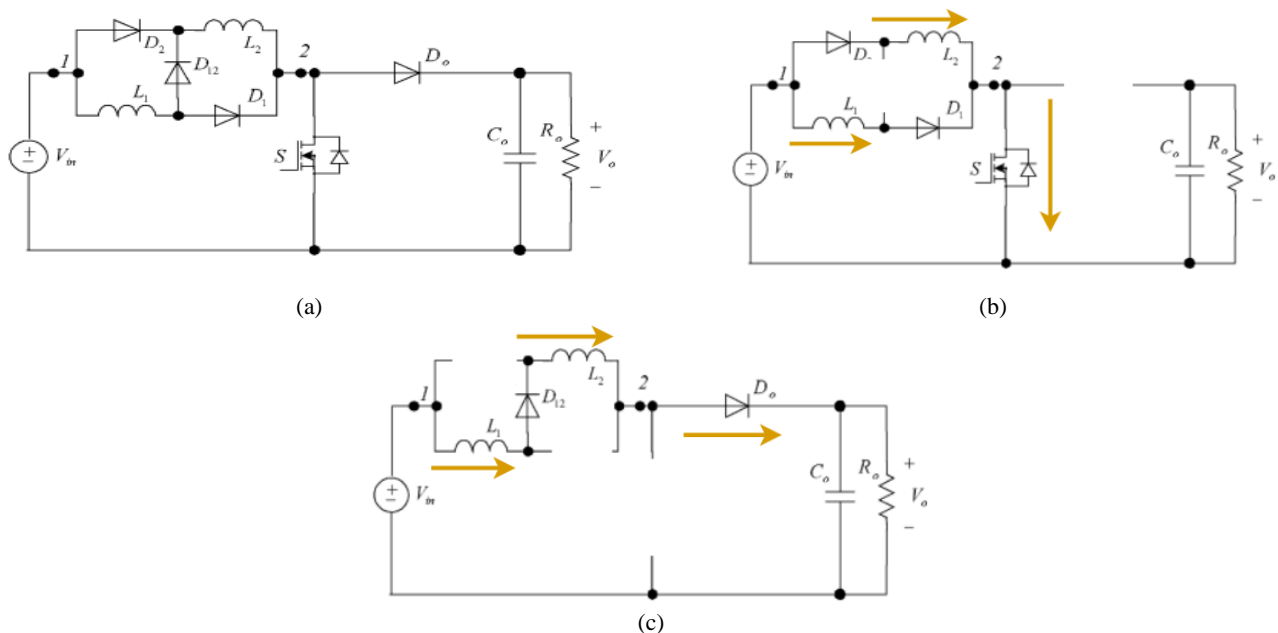


Fig. 4. a) Modified boost equivalent circuit, b) first mode, c) second mode

$V_{in} - V_{L2} - V_{L3} - V_{O} = 0$

(2)

To reduce the ripple;

$V_{L2} = V_{L3}$

$$V_L = (V_{in} - V_O)/2 \quad (3)$$

From the second volt balance

$$V_L T_{on} + V_L T_{off} = 0$$

Then;

$$V_o = v_{in} (1 + D) / (1 - D) \quad (4)$$

To make sure the modified boost act to max lifted voltage with min duty cycle by using equation no 4;

$$V_o = v_{in} (1 + D) / (1 - D)$$

$$V_o = 576(1 + 0.166) / (1 - 0.166) = 805 \text{ v}$$

There are many advantages to operating the boost with a minimum duty cycle:

- Reduce the heating and losses.
- The device operates without a reverse recovery diode [15].

### 3.3.1. Design L&C in DC/DC converter (modified boost)

#### 3.3.1.1. Design L

at S (switch) is on;

$$V_L = V_{in}$$

$$L \Delta I / \Delta T = V_{in}$$

$$L = (V_{in} \times \Delta T) / \Delta I$$

$$L = (V_{in} D T) / \Delta I$$

$$L = (V_{in} D) / \Delta I f_s$$

Where  $T = 1/f_s$

$$\Delta I = 0.05 \times I_o \times V_O / V_{in}$$

#### 3.3.1.2. From Table 1

$$V_{in \text{ dc}} = 28.8 \times 20 = 576 \text{ v}$$

Then,  $V_o / (P_o) = I_o$  where

$$\Delta I = 28.125 \text{ A}$$

$$L = 1.06496 \times 10^{-4}$$

$$\text{At: } f_s = 10 \text{ Kz, } D = 0.55, V_{in} = 576 \text{ v}$$

#### 3.3.1.2. Design C

at S OFF

$$I = \Delta Q / \Delta T, \Delta Q = I \times \Delta T, \Delta Q = I_o(1 - D)T$$

Then;

$$\Delta V_c = \Delta Q / C$$

$$C = (V_o(1 - D)) / \Delta R f_s$$

$$C = 2.4303 \times 10^{-3} \text{ F}$$

## 4. Design and Implementation of the MPPT

The PV system's main feature is the comprehensive monitoring of energy; this permits the PV module's power to be extracted in a specific climatic condition. INC is the most often utilized MPPT algorithm. The INC algorithm at the MMP is based on the idea that The PV output's output voltage power derivative is zero ( $dp/dv=0$ ), positive on the left side of MMP ( $dp/dv>0$ ), The right side of MMP has both positive and bad aspects. ( $dp/dv<0$ ) [16].

The INC algorithm is employed to (see Fig. 5);

The ( $dI/dV$ ) characteristic of the photovoltage system can be used to detect the presence of MPP. The INC-MPPT can be activated by following the steps below [17];

- The MMP controller detects the voltage and current of the PV module.
- If ( $dp/dv, I/V$ ) is met, the duty cycle of the converter must be reduced, and vice versa.
- If  $I+V (dp/dv) = 0$ , there is no change in the duty cycle. from above, the duty cycle (PV reference voltage ( $V_{ref}$ )) increases or decreases.

Many disadvantages appear with utilizing this method from them;

- Slowly in response when calculating or suggesting a new duty cycle.
- High ripple and oscillation in output boost waveform.

To bypass all these issues in the design and Implementation of the MPPT; A comparison has been made to the IC calculation condition algorithm  $\frac{I}{V} + \frac{dI}{dV} = 0$  With set point and treated error signal by fractional PID controller to calculate or suggest a new duty cycle as shown in Fig 6.

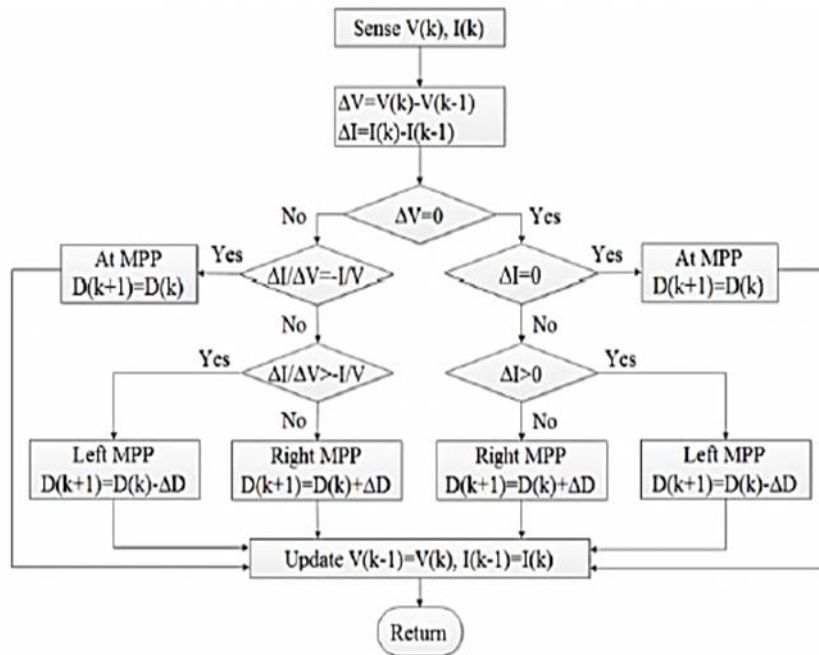


Fig. 5. Flowchart of IC method

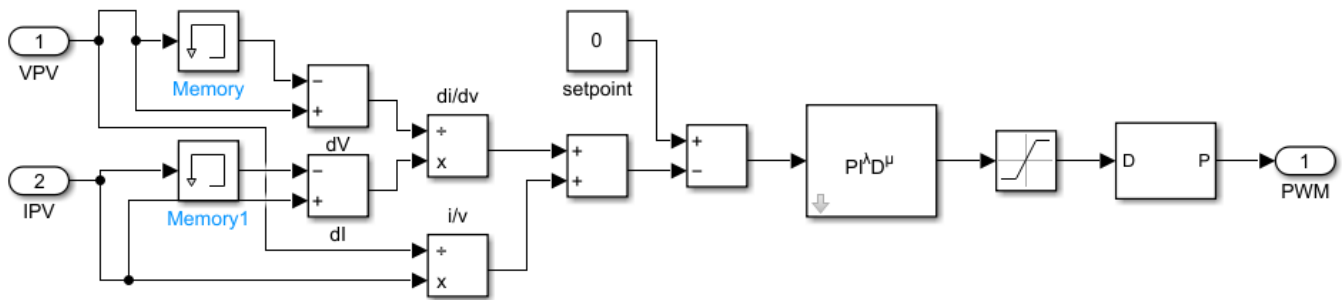


Fig. 6. Implementation simulation of the MPPT

### 5. Cascaded Multilevel Inverter

By linking H-bridge inverters in series, this inverter is designed to output a sinusoidal voltage. The output voltage is the sum of all the voltages generated by the cells. The output voltage has  $2n+1$  levels, where  $n$  is the number of cells. The overall harmonic distortion can be reduced by choosing different switching angles. This type of multilayer inverter has the benefit of requiring fewer components as compared to flying capacitors or diode-clamped inverters., As a result, the inverter is both more affordable and heavier than the other two types. Figure 3 displays the phase lag of the power circuit for five-level cascaded inverter sinewaves used in this investigation. Each single-phase full-bridge inverter in a five-level inverter produces three voltages at the out-put:  $+V_{dc}/2$ ,  $+V_{dc}$ ,  $0$ , and  $-V_{dc}/2$ . To make this possible, the capacitors are connected. The output Ac voltage that generates varies between  $-V_{dc}$  and  $+V_{dc}$  at five different values [18]. The VSI is controlled using a current controlled PWM (CCPWM) approach. The control strategy's major goal is to manage the inverter's current output so that it tracks a reference signal. Multi-loop control is used in the CCPWM approach. The outer loop maintains a constant voltage on the dc connection, while the inner loops manage reactive and active current in a synchronized d-q reference frame aligned with the grid's voltage vector. A phase-locked loop (PLL) method is used to determine the grid voltage vector angle shown in Fig. 7.

By adjusting the active current provided to the inverter, as a reference, the DC link voltage can be kept constant. When the DC link voltage falls below  $V_{dc}^*$ , the regulator lowers the inverter's active current. I ing, causing the capacitor current  $I_c$  to develop in lockstep with the DC link voltage ( $V_{dc}$ ), and vice versa [19].

As a result, the active current component  $I_d^*$  can be referenced using the DC voltage dynamics controller output. The active current recommended by the reference can be described as follows:

$$I_d^* = K_p(V_{dc}^* - V_{dc}) + K_i \int (V_{dc}^* - V_{dc}) dt$$

Where:  $K_p$ ,  $K_i$  controller is a constant.

The voltage and current vectors are measured and transformed in the d-q reference frame at the point of common connection (PCC). the voltage and current vectors become DC quantities due to the d-q synchronous reference frame's constriction, allowing reference current monitoring with 0% steady state error to be achieved with the PI controller [19].

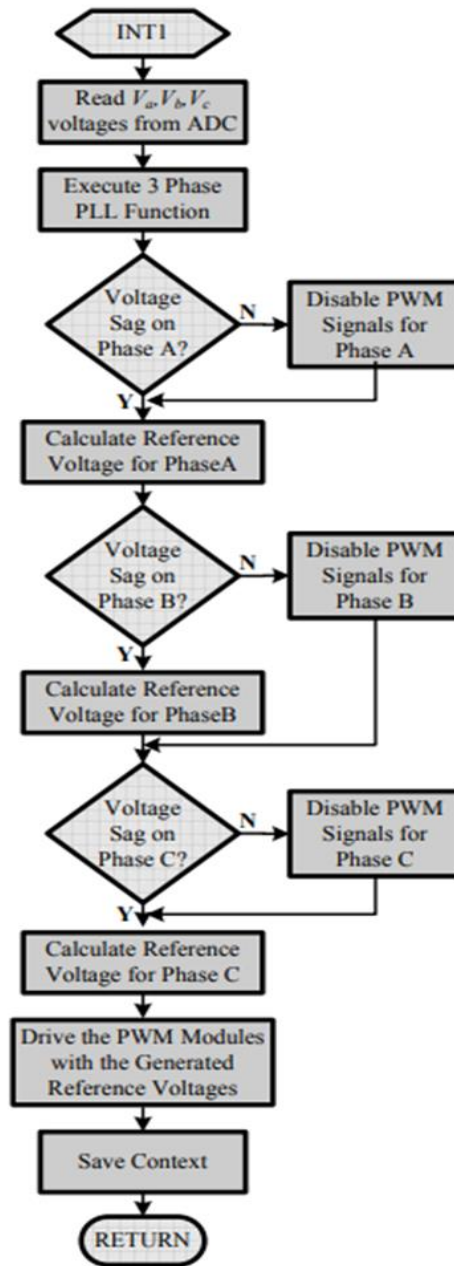


Fig. 7. Flowchart for the PLL algorithm

The inverter's power and voltage equations as shown in Fig. 8 (in d-q frame) are as follows:

$$Vd^* = RI_d + Vd - \omega LI_q + L \frac{d}{dt} I_d$$

$$Vq^* = RI_q + Vd + \omega LI_d + L \frac{d}{dt} I_q$$

$$P = Vd + Id + VqIq$$

$$Q = -VdIq + VqIq$$

A schematic diagram of a grid-connected PV system is shown in Figure 6. a five-level 3 Ø (VSI), filter, transformer for connecting photovoltaic, and a basic distribution system make up the power circuit. A Thevenin equivalent circuit was used to model the utility grid as a three-phase voltage source with series impedances. To represent varying loads in the distribution network, R and RL loads were linked between the photovoltaic system and microgrid [20].

By managing the reactive and active currents separately, the reactive and active power may be adjusted separately. The current component I<sub>q</sub> for the q-axis must be equal to the unity power factor, hence the reactive current component is set to zero. Finally, in the sinusoidal PWM

technique, the command voltage concerning is normalized to the DC link voltage and translated back to the ABC frame to be used as modulating control signals. To generate inverter switch trigger pulses, these signals are compared to a high-frequency carrier [20].

A simulation was done using the MATLAB program to control five-level – three-phase (VSI) as shown in Fig. 9.

By managing the reactive and active currents separately, the reactive and active power may be adjusted separately. The current component  $I_q$  for the q-axis must be equal to the unity power factor, hence the reactive current component is set to zero. Finally, in the sinusoidal PWM technique, the command voltage concerning is normalized to the DC link voltage and translated back to the ABC frame to be used as modulating control signals. To generate inverter switch trigger pulses, these signals are compared to a high-frequency carrier [20].

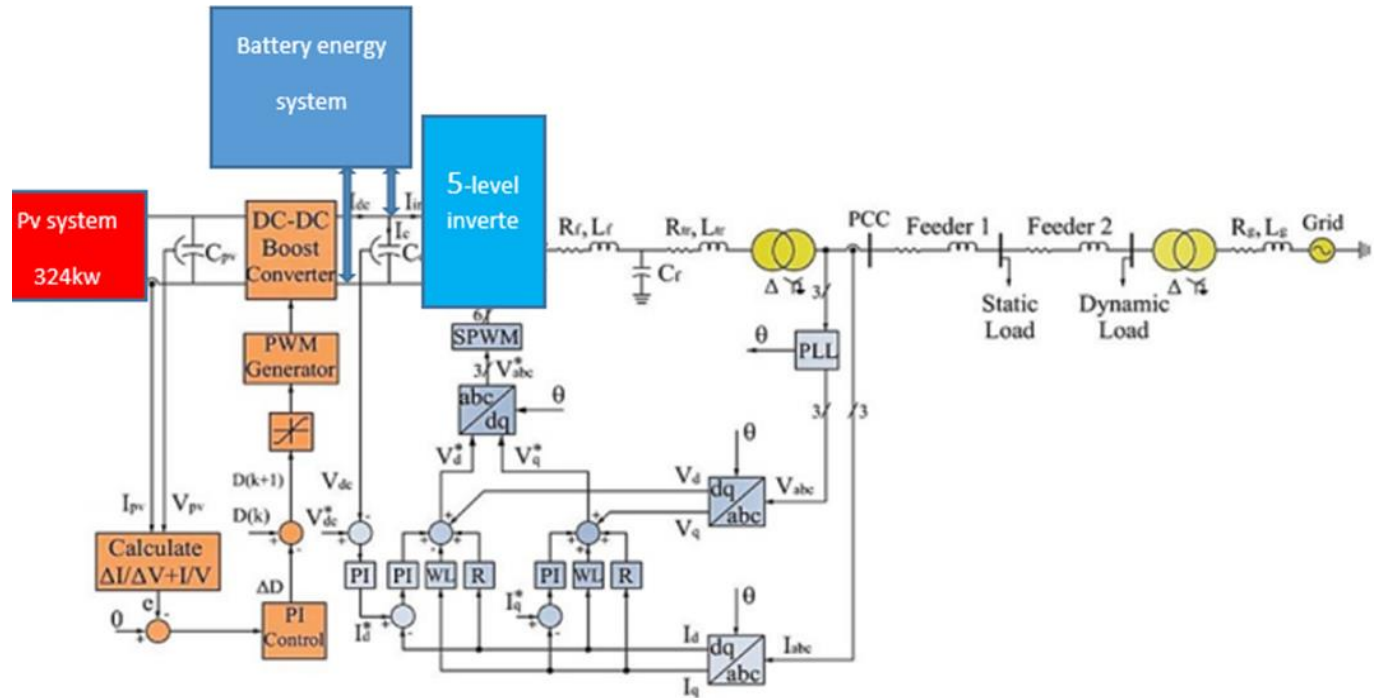


Fig. 8. The Grid Connected PV Schematic Diagram with five level VSI Control [19]

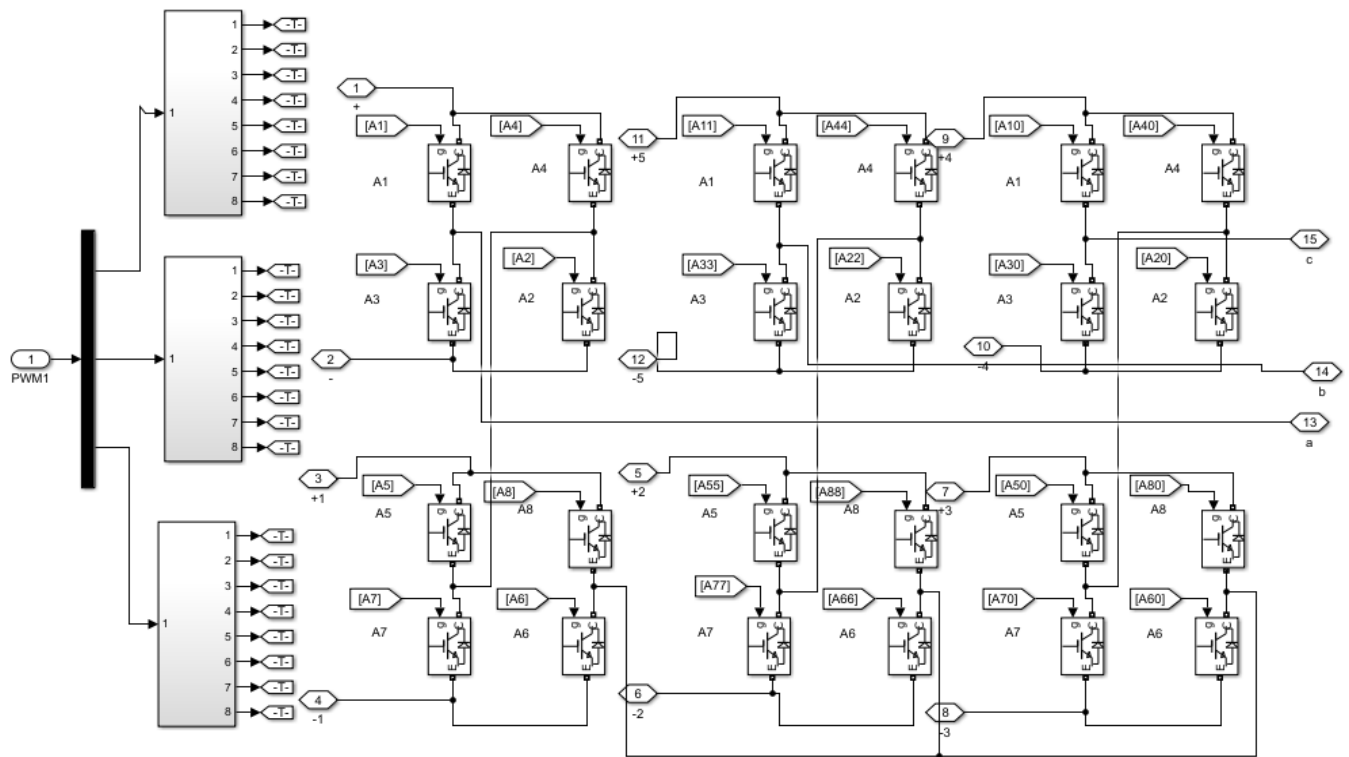


Fig. 9. Simulation circuit of the 3-phase 5-level multilevel

6. Simulation Results

The suggested control method for the photovoltaic system was developed and evaluated using MATLAB/SIMULINK at various solar insolation levels. To depict the transient reaction of the suggested control system, PV insolation is assumed to increase from 500 to 700 W/m<sup>2</sup> at 1 s, 700 W/m<sup>2</sup> to 1000 W/m<sup>2</sup> at 2 s, and decrease from 1000 to 500 W/m<sup>2</sup> at 3 s. The temperature was chosen to be (25, 45, 65) °C. To evaluate how reliable, the proposed control mechanism is, an abrupt increase or reduction is assumed in this work. Under the aforementioned operating conditions, the revised boost converter's inductor current is modulated to track the MPP correctly, and the power flow between the multilevel inverter, microgrid, and static, dynamic load is also changed. Using the IC MPPT algorithm and FOPID, Fig. 10 shows the enhanced boost converter's dynamic performance. The IC MPPT algorithm and FOPID are used to calculate the duty cycle as a result of a variable PV voltage and current proportional to the modified boost. The PV characteristics are shown in Fig. 10 at three insolation levels the highest possible power ampere and volt are 160 kW, 280 A, and 576 V. The updated boost converter is utilized to track these values in Fig. 11 (a & b). For the aforementioned operating insolation levels, tracked values for photovoltaic kW, volt, and ampere are shown in Table 3. These results show that the improved boost converter is monitoring the maximum power.

The multilevel inverter (5-level) is actively controlled to inject the high equality active power as well as to rectify the THD and Kvar required by the unbalanced and non-linear load at PCC to guarantee that the current drawn from the grid at UPF is only sinusoidal. With fluctuating solar radiation and nonlinear unbalanced load currents, as well as the voltage and current waveforms leaving the inverter at PCC, the performance of the multilayer inverter's dynamic compensation using the recommended control algorithm, the inverter voltage waveform did not change throughout the transient, but the amplitude of the earlier inverter waveforms did as a result of the quick shift in PV brought on by the total harmonic distortion of 2.4, as seen in Fig. 12. (a & b).

There are two quantities of loads have been equipped and connected. The first quantity is 180 kW connected directly, and the second quantity is 100 kW shown in Fig. 13. It enters the system within 2 to 3.5 seconds along with grid side currents. voltages and current waveforms coming out of the inverter at PCC.

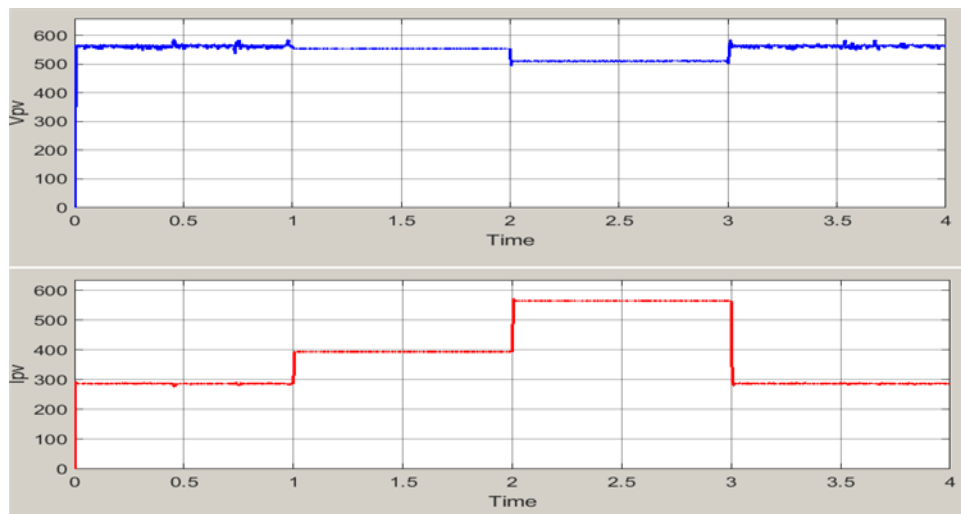
Table 3 shows the greatest power gathered from PV arrays with insolation  $G = 500 \text{ W/m}^2, 700 \text{ W/m}^2, \text{ and } 1000 \text{ W/m}^2$ . Electricity can be seen to flow from the dc side to the ac link before supplying the ac load. The dynamic performance of power flows between a PV system, the grid, and the load is shown in Fig. 14.

PV systems face several obstacles and challenges, the most important of which are:

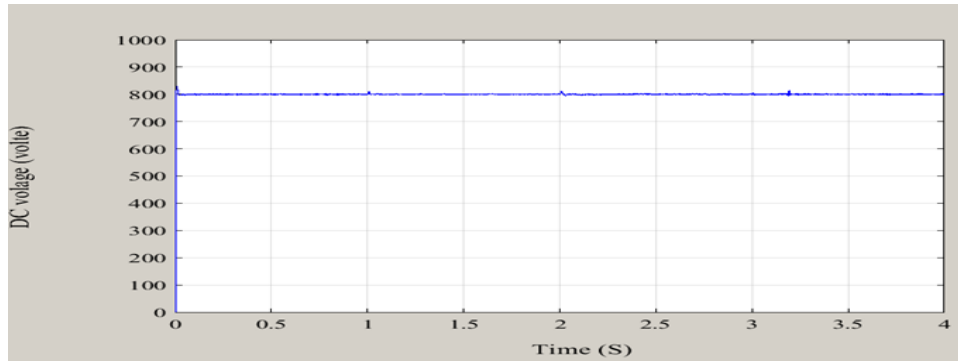
- Absurdly high costs associated with the development, upkeep, and storage of systems such as hydropower to store with pumping, batteries, and compressed air to ensure that power is continuously supplied.
- Additional transportation, maintenance, and service costs must be incurred because specialized engineering expertise may not be available, which is especially problematic in remote locations.
- Protection, control, and assurance of power supply to consumers in island mode.
- When changing operating points to generate load-matching frequencies in island mode, consider power quality, frequency, and voltage

Table 3. Maximum power tracking performance

Time(s)	G ( W/m <sup>2</sup> )	Temperature (C <sup>o</sup> )	V	A	P pv max(kW)
0 - 1	500	25	576	280	160
1 - 2	700	45	550	400	220
2 - 3	1000	65	505	560	283
3 - 4	500	25	576	280	160

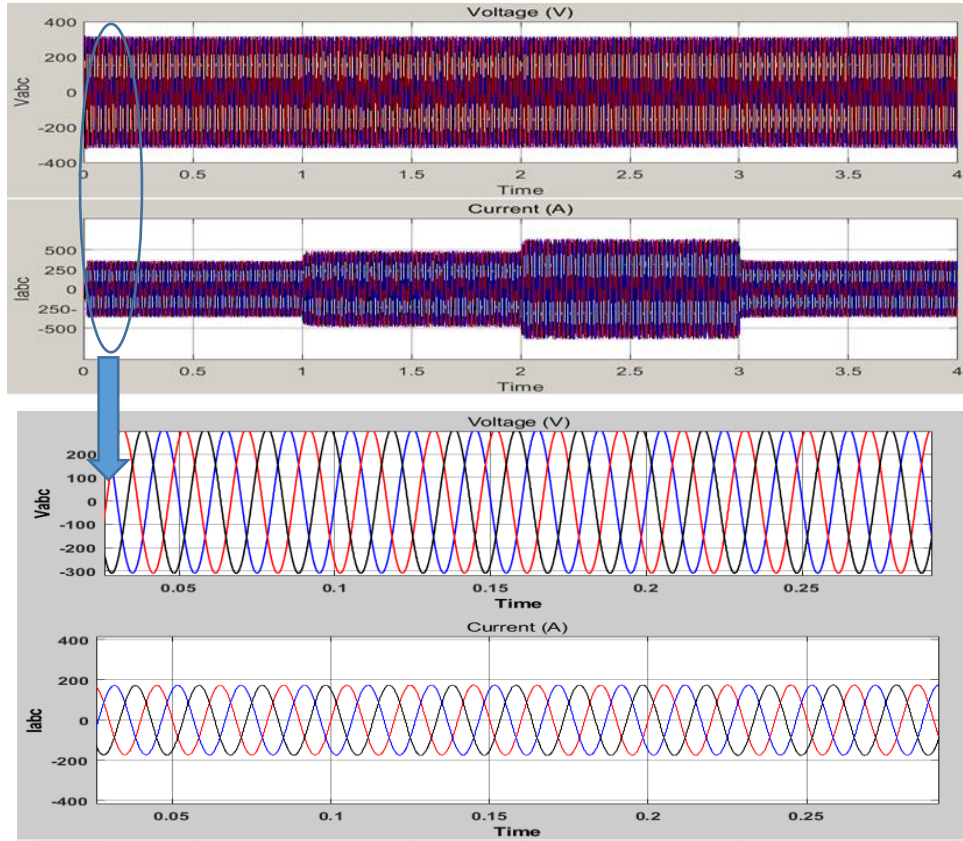


(a)

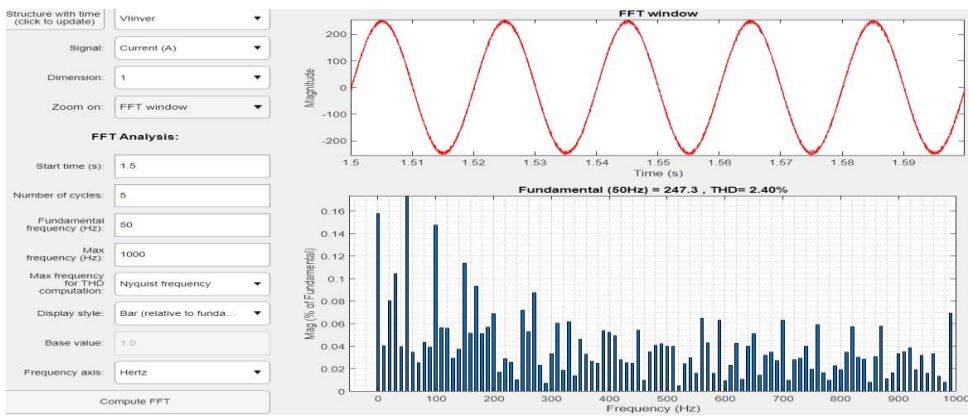


(b)

Fig. 10. A. Terminal current, the voltage of PV panel b. DC link voltage



(a)



(b)

Fig. 11. (a) Inverter Waveform, (b). Total Harmonic Distortion

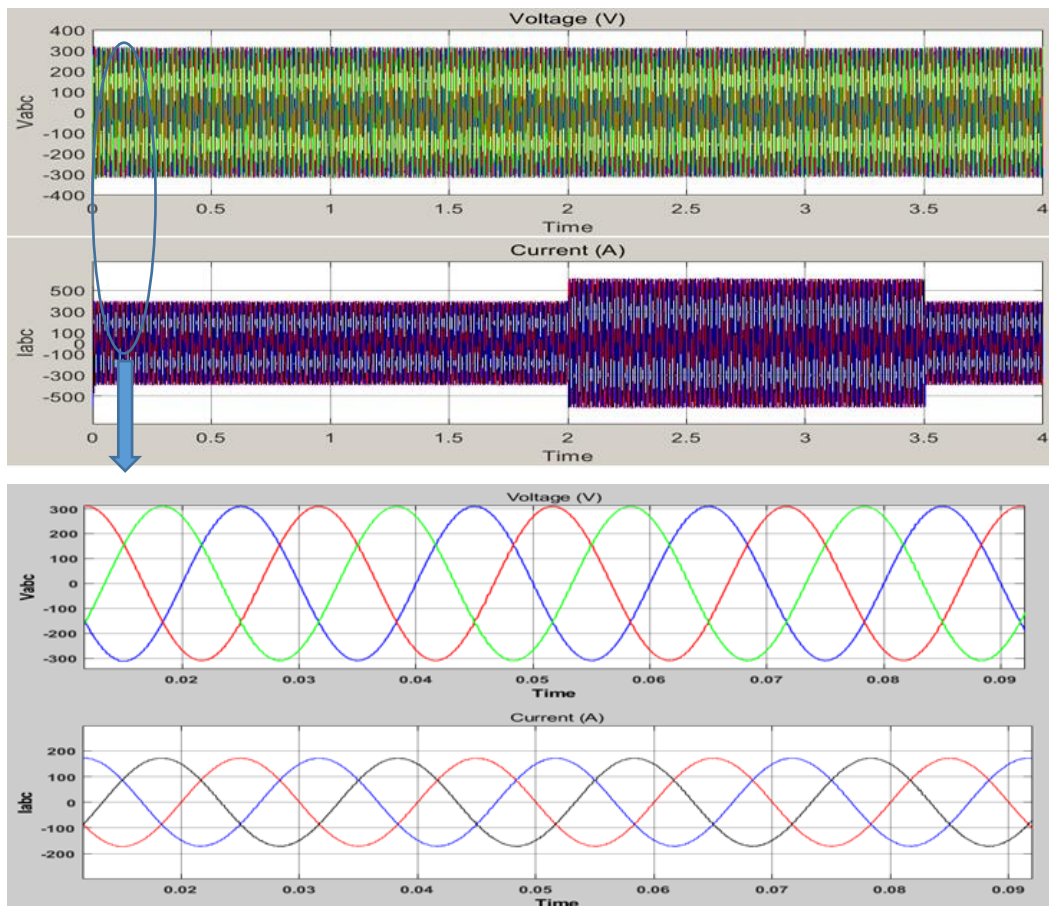


Fig. 12. Voltage and Current of Load

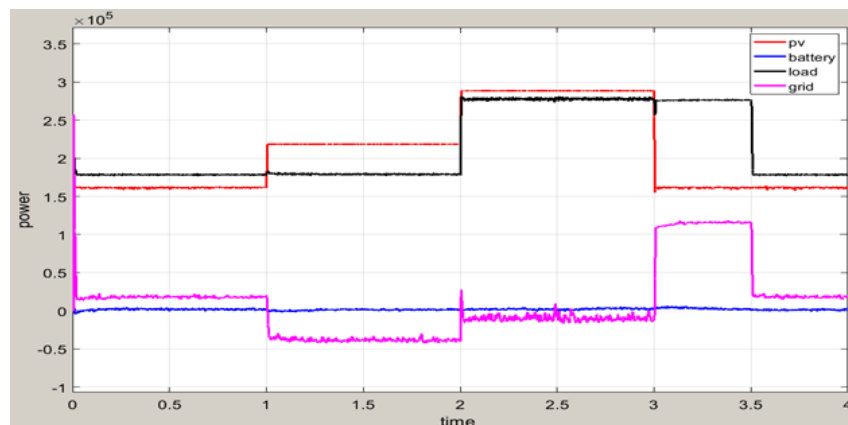


Fig. 13. Power of the system

## 7. Conclusion

It has been demonstrated that a 324 kW PV system connected to the grid performs well thanks to the application of the MPPT to the multilevel inverter (five levels) proposed in this work. Also offered is a good control strategy for the MPPT and inverter. A modified boost act to track the MPPT (IC method with FOPID) with minimal losses, heating, and current ripple. The multilevel inverter can simultaneously inject high-quality AC power into the grid and use harmonic and reactive power to balance out uneven static and dynamic demand loads at (PCC). The system operates flawlessly in a changing environment. The simulation results show that the multilevel inverter can function with a current THD of 14% under an imbalanced nonlinear load.

## Acknowledgment

I owe my deepest gratitude to Electrical Engineering Technical College, Middle Technical University for their support, guidance, and encouragement throughout this work.

## Reference

- [1] Naderipour, A., et al. Control method for three-phase grid-connected inverter PV system employing unity power factor (UPF) strategy in a microgrid. in E3S Web of Conferences. 2019. EDP Sciences.
- [2] Faicel El Aamri, H. Maker, A. Mouhsen, M. Harmouchi . A new strategy to control the active and reactive power for single-phase grid-connected PV inverter. Engineering. 2015 3rd International Renewable and Sustainable Energy Conference (IRSEC). 2015.
- [3] Amirreza Naderipour, Zulkurnain Abdul-Malek , Vigna K. Ramachandaramurthy and Josep. M. Guerrero ." Control Method for Three-Phase Grid-Connected Inverter PV System Employing Unity Power Factor (UPF) Strategy in Microgrid". CEEGE. 2019.
- [4] Syed Muhammad Ahsan, Hassan Abbas Khan, Akhtar Hussain, Sarmad Tariq and Nauman Ahmad Zaffar " Harmonic Analysis of Grid-Connected Solar PV Systems with Nonlinear Household Loads in Low-Voltage Distribution Networks". Sustainability. 2021.
- [5] Chokchai, C. Power flow control and MPPT parameter selection for residential grid-connected PV systems with battery storage. in 2014 International Power Electronics Conference (IPEC-Hiroshima 2014-ECCE ASIA). 2014. IEEE.
- [6] Phani Kumar Chamarthi, Ahmed Al-Durra, Khaled Al Jaafari" A Novel Three-Phase Transformer less Cascaded. Multilevel Inverter Topology for Grid-Connected Solar PV Applications" IEEE Transactions on Industry Application. 2021.
- [7] Henry Benedict Massawe ". Grid Connected Photovoltaic Systems with Smart Grid functionality". Engineering. Published. 2013.
- [8] Ali Bouhafs, Bendaas Mohamed Lokmane, DJARALLAH Mohamed ". Grid-connected photovoltaic system, for an 800 W ". Engineering. ScienceDirect. 2015.
- [9] Ayachi Amor Nourdine, Ayachi Amor Yacine, Kheldoun Aissa, Metidji Brahim " Comprehensive Modeling and Simulation of Grid-Tied PV System". Boumerdes (ICEE-B) . 2017.
- [10] Amirreza Naderipour, Zulkurnain Abdul-Malek , Vigna K. Ramachandaramurthy and Josep. M. Guerrero. " Control Method for Three-Phase Grid-Connected Inverter PV System Employing Unity Power Factor (UPF) Strategy in Micro grid" CEEGE 2019.
- [11] Aravind Khote, Asst. Prof. Ms. Shalini Goad. " A Comparative Study on Maximum Power Point Tracking Techniques for Utility Grid Connected Photovoltaic Systems using ANFIS and INC Method " International Journal of Scientific Research & Engineering Trends 2021.
- [12] Dalila Beriber, Abdelaziz Talha, "MPPT techniques for PV systems", 4th International Conference on Power Engineering, Energy and Electrical Drives, 10.1109/PowerEng.2013.6635826, 20131993.
- [13] M. Vinay Kumar, U. Salma " Modeling And Simulation Of A Three Phase Grid Connected Photovoltaic System". European Journal of Molecular & Clinical Medicine. 2020.
- [14] Weidong Xiao. "power electronic step-by-step design, modeling simulation, and control". 2021.
- [15] Alex Stanley Raja Thaveedu, Senthil Kumar Ramaswamy and Shiva Prakash Thirumurugan "PV-Wind-Battery based Bidirectional DC-DC Converter for Grid Connected Systems". IOP Conference Series: Materials Science and Engineering. 2020.
- [16] S. Motahhir, A. El Ghzizal, S. Sebti, and A. Derouich, "Modeling of a photovoltaic system with modified incremental conductance algorithm for fast changes of irradiance," International Journal of Photoenergy, vol. 2018.
- [17] R. Pradhan, S. Pradhan, and B. B. Pati, "Design and performance evaluation of fractional order PID controller for heat flow system using particle swarm optimization," in Computational Intelligence in Data Mining, pp. 261–271, Springer, Cham, Switzerland, 2019.
- [18] Bindeshwar Singh, Nupur Mittal, Dr. K.S. Verma, "Multi-Level Inverter: A Literature Survey On Topologies And Control Strategies" International Journal of Reviews in Computing, 2019.
- [19] Humaidi, A.J., A.H. Hameed, and M.R. Hameed. Robust adaptive speed control for DC motor using novel weighted E-modified MRAC. in 2017 IEEE International Conference on Power, Control, Signals and Instrumentation Engineering (ICPCSI). 2017. IEEE.
- [20] Bairwa, A.K., S. Joshi, and D. Singh, Dingo Optimizer: A Nature-Inspired Metaheuristic Approach for Engineering Problems. Mathematical Problems in Engineering, 2021. 2021.